Cold Tests and Magnetic Characterization of a Superconducting Magnet for a Compact Cyclotron for Radioisotope Production

Javier Munilla, Pablo Abramian, Miguel J. Barcala, Jesús Calero, Manuel Domínguez, Antonio Estévez, Luis García-Tabarés, José L. Gutiérrez, Daniel López, Diego Obradors, Fernando Toral, Cristina Vázquez, Rafael Iturbe, José Gómez, Fulvio Becheri, Josep Campmany, and Llibert Ribó

***Abstract*—A superconducting magnet able to provide the required field of 4 T has been developed for a compact cyclotron to produce radioisotopes for medical imaging, in the framework of the AMIT project. It consists of two coils in Helmholtz configuration, embedded in a stainless steel casing to hold the Lorentz forces. The cooling scheme is based on a low pressure forced internal flow of two-phase liquid-vapour helium through a narrow channel machined in that casing. This paper reports on the cooling tests and the preliminary magnetic measurements of the magnet. Regarding cooling tests, liquid Helium from a Dewar has been used first to train the magnet and to estimate the thermal losses. Later, refrigeration will be accomplished from a stand-alone cryogenic supply system that would allow a user-friendly operation of the cyclotron, without external supply of cryogens. Regarding magnetic measurements, a custom magnetic measurement bench developed in collaboration with ALBA/CELLS, has been used to map the magnetic field and first results are presented and discussed in this paper.**

***Index Terms*—Compact cyclotrons, cryogenics, magnet, radioisotope.**

I. Introduction

POSITRON Emission Tomography (PET) technique is broadly used around the world as a diagnostic tool and also as a medical treatment [1].

Compact cyclotrons which allow producing single doses of short-life isotopes for sintering PET radiotracers are becoming an alternative to their fabrication in large production centers and also a real demand from medical institutes [2]. They will satisfy the requisites for non-standard PET demands which need to be produced close to where they are used, based on an accelerator which provides the minimum required energy and current with a reduced footprint [3]. In 2010, the AMIT project (Advanced Molecular Imaging Technologies) was started as a multilateral collaboration of Spanish institutes and industries, initially led by SEDECAL. The project has been funded from different governmental and private sources and it included the development of a compact cyclotron for single dose production of ^{18}F and ^{11}C, a Lawrence type machine accelerating H^- up to an energy of 8.5 MeV and a current of 10 μA [4].

The cyclotron is based on a NbTi superconducting magnet producing a nominal field of 4 T and it is cooled down with two-phase helium circulating in a closed circuit, which is recondensed externally later. Main components of the accelerator have already been finished and are now under testing and commissioning.

Fig. 1 shows a general overview of the cyclotron magnet ready for the tests, including the magnetic test bench [5] and the alignment system.

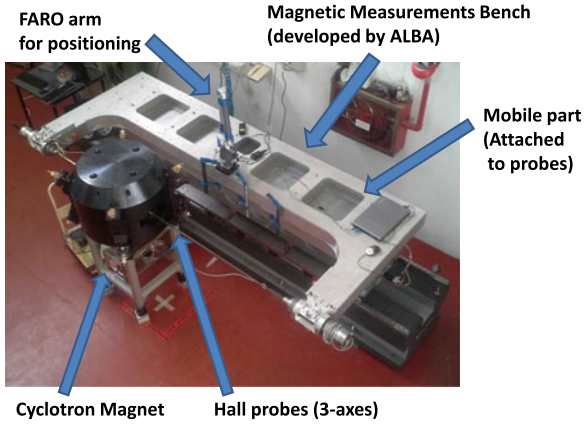

Fig. 1. Cyclotron magnet, magnetic test bench and alignment system for magnetic characterization.

II. Assembly

A. Cyclotron Interfaces and Testing Assembly

Magnet design and assembly was described in a previous work [6]. A brief summary including the most important values

Manuscript received August 28, 2017; accepted October 27, 2017. Date of publication November 20, 2017; date of current version December 8, 2017. This work was supported in part by the Spanish Ministry of Economy, Industry, and Competitiveness under project FPA2016-78987-P. *(Corresponding author: Javier Munilla.)*

J. Munilla P. Abramian, M. J. Barcala, J. Calero, M. Domínguez, A. Estévez, L.García-Tabarés, J. L. Gutiérrez, D. López, D. Obradors, F. Toral, and C. Vázquez are with CIEMAT, Madrid 28040, Spain (e-mail: javier.munilla @ciemat.es).

R. Iturbe is with ANTECSA, Portugalete 48920, Spain.

J. Gómez is with Vacuum Projects, Paterna 46988, Spain.

F. Becheri, J. Campmany, and L. Ribó are with ALBA, Cerdanyola 08290, Spain.

Color versions of one or more of the figures in this paper are available online at http://ieeexplore.ieee.org.

Digital Object Identifier 10.1109/TASC.2017.2775582

TABLE I
CYCLOTRON SUPERCONDUCTING MAGNET PARAMETERS

Parameter	Value
Magnetic Central Field	4.00 T
Magnetic Field Radial Gradient @ r = 105 mm	1.49%
Nominal Current	108.6 A
Self Inductance (Both Coils) @ Nom. Current	38.35 H
Thermal Losses at Cryocooler First Stage	34 W
Thermal Losses at Cryocooler Second Stage	0.7 W

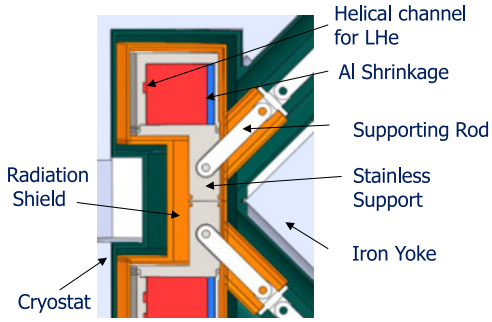

Fig. 2. Coil, cryostat and support structure cross section.

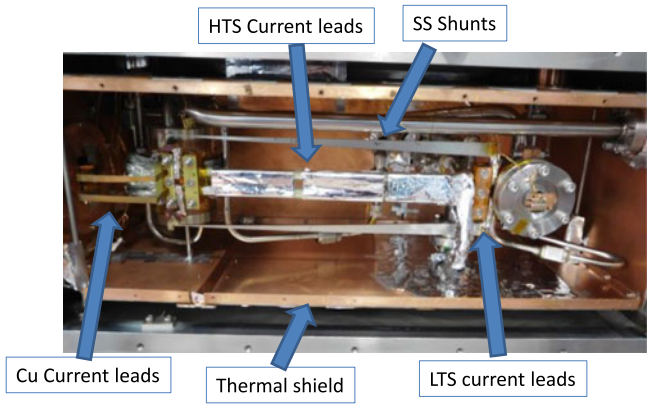

Fig. 3. Connection box assembly and its main components.

about the magnetic and thermal design can be found in Table I. Fig. 2, which is also extracted from [6], shows the conceptual design of the magnet. G10 rods are supporting the coils and the casing inside the cryostat, while a thermal shield is needed to reduce the thermal losses from both, radiation and conduction, from ambient temperature cryostat walls.

Nominal operation conditions of the cyclotron magnet include an autonomous reliquefaction system (CSS) for providing liquid Helium (LHe) and gas Helium (GHe) at 40 K. These two cryogens will be transferred from the CSS to the cyclotron by means of a custom low loss transfer line, as explained in [7].

Connection from the transfer line to the magnet is performed by a connection box shown in Fig. 3. This connection box includes the interfaces for the cryogens distribution to both refrigeration circuits inside the magnet, the current leads for powering the magnet and some of the safety devices for operation and quench protection. Pipes transferring the cryogens are connected by Kenol fittings for an easy dismantling.

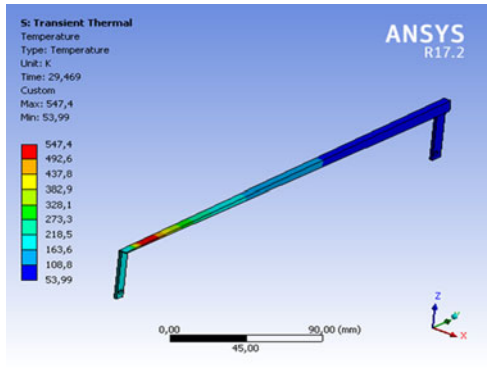

Fig. 4. Maximum temperature value at current lead shunts under pessimistic scenario (30 s after a complete quench on the HTS current lead, adiabatic constraints and nominal current 110 A).

Current leads are refrigerated just by conduction, and include three different steps. Two copper leads are connecting the room temperature feedthrough in the cryostat wall to the warm side of a high-temperature superconductor current lead (Cryosaver HTS-110, 150 A). This connection is also refrigerated by a heat exchanger fed by the GHe circuit. The cold side of the current lead is thermally anchored to a small LHe reservoir at the right side of the Fig. 3. Finally, NbTi wires are going inside the LHe pipe by means of a custom low-temperature feedthrough in the previous reservoir.

For safety reasons, in case of a quench in the current leads, two shunt resistors are mounted in parallel to the HTS current leads. The electro-thermal design of these shunts was carried out to minimize thermal losses at the low temperature side, while providing enough electrical conductivity to achieve overtaking the magnet current during the discharge of the magnet. Finally, their cross-section area was designed to achieve thermal losses below 40 mW (for both shunts). Fig. 4 shows the maximum temperature at the most pessimistic condition. That is considering a quench in the current lead at nominal current and adiabatic constraints in the shunt. There is a local hot spot in the shunt because the Joule heating exceeds the heat diffusivity capability. Maximum value occurs at about 30 s after quenching. As Joule heating decreases because the current decays through the dump resistor, heat generation drops and distributes more uniformly along the shunt.

The connection box also includes all the sensor wires and the piping needed for cryogen distribution. Every part to be cooled down to 4.5 K is surrounded by another thermal shield refrigerated by the same gas circuit (series arrangement) and covered by low absorptance insulation.

Finally, high vacuum level is needed to minimize gas conduction from the cryostat and thermal shield to the casing. A turbomolecular pump is connected to the connection box, providing a vacuum level between 10^{-6} to 10^{-7} mbar, which is required at cryogenic temperatures.

During the tests presented in this paper which include standalone characterization of the magnet, liquid Nitrogen (LN) and LHe from Dewar storages will be used. Because of that a customized transfer line was manufactured. Fig. 5 shows the setup for the thermal characterization of the magnet.

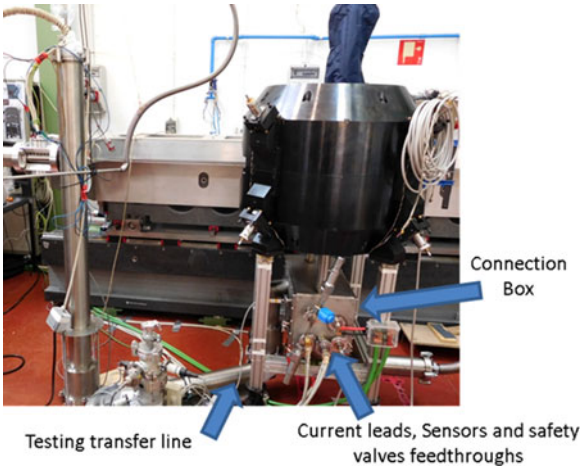

Fig. 5. Cyclotron magnet and transfer line for thermal characterization using external cryogens from a Dewar

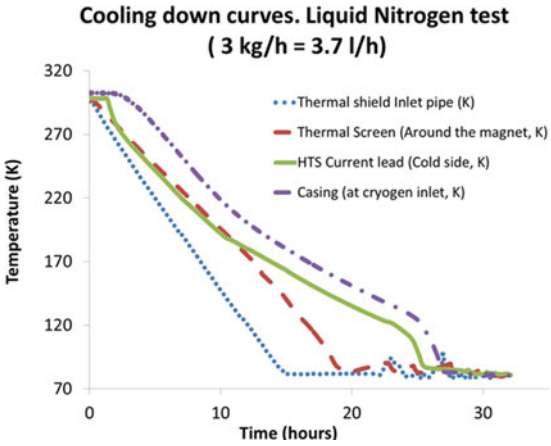

Fig. 6. Cooling down curves using liquid Nitrogen.

III. Liquid Nitrogen Test

Initial tests to characterize the thermal performance of the cyclotron magnet were done by cooling it down with LN from a pressurized Dewar and controlling the mass flow with a controller placed at the outlet, just before the warm exhaust Nitrogen is vented. In this configuration, liquid cryogen is injected to the casing through the connection box and then it refrigerates the cold end of current leads. After that it is circulated to the thermal shield and warm end of current leads before reaching the outlet to ambient.

Refrigeration capability of the casing cooling channel and the heat exchangers was experimentally verified [8]. Cooling down process, steady-state temperature and flow provide important data on the thermal performance of the cyclotron in a cheap and easy test compared to using LHe as cryogen. With this test, the achievement of the superconducting state at the current leads can also be verified while its main limitation is that the coil is not able to become superconductor. Fig. 6 shows cool down curves, according to the expected values in terms of time and cryogen flow requirements (29 h expected for 3 kg/h LN flow, instead of 27 h). Steady state is reached when the liquid reaches the casing which has the greatest heat capacity of the circuit.

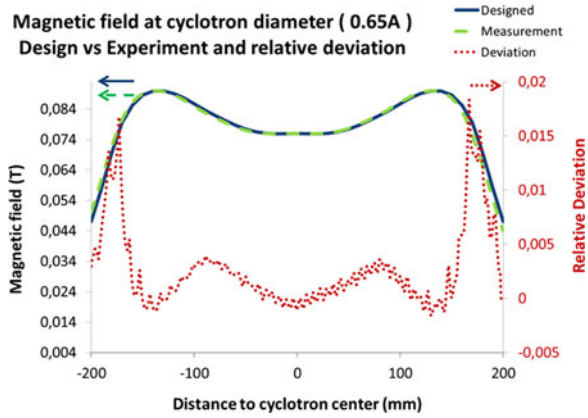

Fig. 7. Magnetic field at centered diameter (0.65 A).

Additionally, this test allows another interesting measurement. Since the coil is fully immersed in LN and its electrical resistance decreases with the temperature, cooling the magnet down with LN allows to power the coil, in a non-superconducting state, up to 0.65 A, a limit given by the maximum voltage that the power supply is able to provide, 150 V. Although this current is really small compared to nominal current, it allows checking the magnetic field map at very low currents, which provides valuable information from the point of view of model verification.

An important point about this magnetic measurement is to set the procedure on the alignment and reference frames between the magnet and the test bench. This procedure was carried out by using a FARO Arm attached to the mobile part of the test bench, so that the magnet was measured at different positions and the information was correlated to the internal encoders of the test bench. This allows knowing not only the translation vector from sensor absolute position to magnet measuring point but also the rotation matrix from one coordinate frame to the other.

Fig. 7 shows the magnetic field distribution for 0.65 A comparing simulated and measured values. Deviation is less than 0.5 % for any position in a centered circle of 150 mm diameter.

IV. Liquid Helium and Superconducting Test

Once the magnet and the set-up were checked down to LN temperature including the control system, the sensors and the valves, a test at liquid helium was carried out.

After precooling the magnet with LN, the Nitrogen was removed and then cleaned with gas Helium and vacuum alternatively. Then, LHe from a pressurized Dewar was injected into the system through the transfer line. The flow was controlled by mass flow controllers at the outlet in a similar way as it was done in the previous test with LN. The amount of LHe required and the cool down curves were measured and stored to evaluate the thermal performance of the system.

Once the temperature was stabilized, the magnetic measurements were performed. Current was increased by steps, measuring magnetic field at some points for each current value. This strategy allowed checking the magnetization properties of the iron and its effects on the real magnetic field in the mean plane

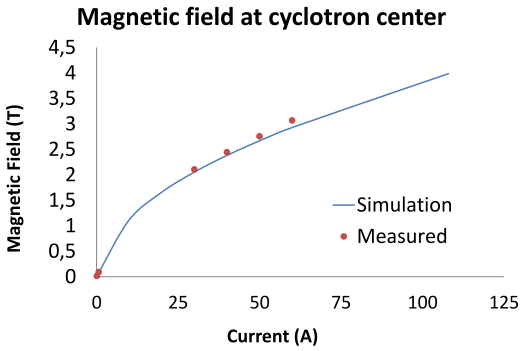

Fig. 8. Magnetic Field Value at Cyclotron Center as function of coils current.

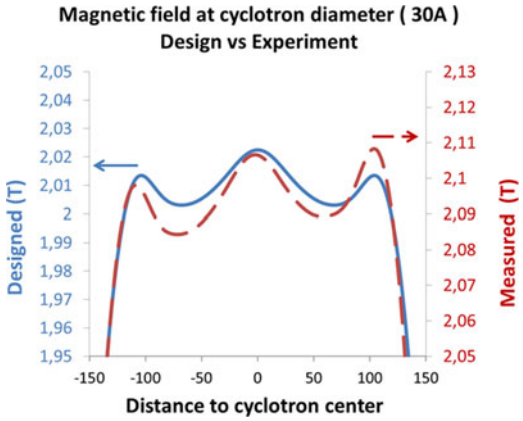

Fig. 9. Magnetic field at cyclotron diameter, 30 A.

of the cyclotron. Fig. 8 shows the magnetic field measured in the center of the cyclotron compared to the simulation values. Measured values for magnetic field at magnet center are slightly bigger. Iron properties were measured just up to 2 T and magnetic test bench was calibrated up to 2 T, so these values are extrapolated and this could be the reason for this difference.

Regarding the magnetic field mapping of the iron, it was first performed at 30 A, and some interesting results were drawn. Not only the absolute value of the magnetic field is different when comparing powering the magnet at 30 A or at nominal current, but also the shape differs slightly. This small difference on the field shape and particularly on the fact that the magnetic field at the center is not a global maximum value represents a major difference in terms of particles stability. This means that higher values of current are needed not only to reduce the bending radius of the particles, but also to achieve beam stability [9].

Another important check to be done is to confirm the azimuthal symmetry of the magnetic field. It will greatly affect beam stability and beam current reaching the target. Fig. 9 shows the magnetic field at 30 A at a cyclotron diameter in the mean plane. While nominal curve is fully symmetric, the measured curve shows a 0.5 % deviation on this symmetry. As particles will be moving in circular paths, they will feel alternative oscillations on the magnetic field at a given radius and this should be considered for the beam dynamics and its stability [9]. It can be easily proved by simulations that the real position of the coils cannot explain this effect, so the iron properties, its dimensional accuracies and misalignment measurements between hall

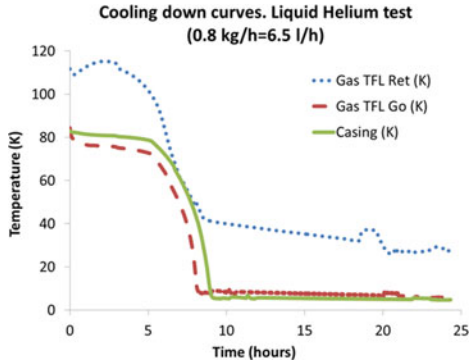

Fig. 10. Cooling down curves using liquid Helium.

probes and cyclotron magnet should be the reason for this non symmetrical behavior.

When increasing the current to higher values, some problems aroused related to the alignment and supporting system of the coils, so 65 A was the maximum testing current value for safety reasons.

In order to validate mechanical and thermal concepts, a previous test was carried out in the past [8], and now a complete real test was performed on the thermal behavior of the cyclotron. Refrigeration principle was the same as for the nitrogen test, and helium was provided from a pressurized Dewar.

Fig. 10 shows the cooling down curve when using LHe and the amount of helium required for it. Expected time needed for a 0.8 kg/h flow was around 11 h, while casing reached liquid temperature in just 10 h. It is important to notice that the two cooling circuits are directly connected, so temperatures at the second stage are lower from expected at real conditions. Also, the helium enthalpy is not used, as exhaust helium gas is at 34 K. At nominal conditions using the CSS, this enthalpy will be recovered by precooling the injection helium gas to the cryocooler.

Steady-state conditions were achieved when the whole magnet circuit was full with liquid Helium up to the input pipe of the second circuit in the cyclotron. Helium temperature at the outlet of the cyclotron was 34 K allowing to calculate the enthalpy change of the Helium used for refrigerating the magnet, resulting in an overall power of 31 W, while the design value was 34 W. It is also important to notice that now the temperature distribution is not the same, since the second circuit is cooled with liquid helium instead of being cooled with gas helium at 40 K as it is when using the CSS [10] and that during cool down process there is no current through the current leads. Future tests will be aimed at separating the power requirements for each circuit from the helium quality factor data coming from the first circuit.

It is foreseen to reach the steady-state for which the complete first circuit is at helium evaporating temperature. From the required helium flow, losses at the primary circuit can be determined.

V. Conclusions

Compact cyclotrons are arising an increasing interest for the production of single doses of radioisotopes. The only way for

reducing the sizes of the cyclotron is increasing its magnetic field leading to the use of superconducting magnets.

This paper has presented results concerning thermal and magnetic design and testing of the AMIT Cyclotron (based on a 4 T NbTi magnet working at 4.5 K) as part of a testing campaign of different accelerator subsystems.

It includes information on the measured magnetic field shape compared to the design values, and the thermal heat losses when cooled with cryogens from a Dewar. Both magnetic and thermal tests result in good agreement with simulation and design values. The magnet was also driven to the superconducting state reaching a magnetic field up to 3 T, which was also recorded. Further measurements to nominal field will require new mechanical adjustments.

Further work to be done include the modifications on the CSS system in order to optimize the cooling down time. It will also allow testing the accelerator in real and autonomous working conditions without additional cryogens. Magnetic field will be recorded up to nominal value and possible adjustments for quality improvements are foreseen.

REFERENCES

[1] "FDA approves 11C-choline for PET in prostate cancer," *J. Nucl. Med.*, vol. 53, no. 12, p. 11N, Dec. 2012.

[2] U. Zetterberg, "A_change_in_usage_of_cyclotrons_for_medical_web.pdf," *presented at theCompact Accelerators for Isotope Production Workshop*, Cockcroft Institute, Warrington, U.K., 2015.

[3] D. M. Lewis, "Accelerator-driven Production of Medical Isotopes," presented at the Cockcroft Institute, Warrington, U.K., 2011.

[4] F. Toral, "The AMIT cyclotron magnet." in *Proc. Panel Rev. Meet.*, Madrid, Spain, 2012, pp. 3–15.

[5] J. Campmany, L. Ribó, C. Colldelram, F. Becheri, J. Marcos, and V. Massana, "A new bench concept for measuring magnetic fields of big closed structure," *Phys. Procedia*, vol. 75, pp. 1222–1229, Jan. 2015.

[6] L. García-Tabarés *et al.*, "Development of a superconducting magnet for a compact cyclotron for radioisotope production," *IEEE Trans. Appl. Supercond.*, vol. 26, no. 4, pp. 1–4, Jun. 2016.

[7] F. Haug, "The AMIT magnet cryosystem." in *Proc. Panel Rev. Meet.*, Madrid, Spain, 2012, pp. 10–12.

[8] J. Munilla *et al.*, "Validation test of the forced-flow cooling concept for the superconducting magnet of AMIT cyclotron," *IEEE Trans. Appl. Supercond.*, vol. 26, no. 3, Apr. 2016, Art. no. 4401204.

[9] C. Oliver, "Optimizing the radioisotope production with a weak focusing compact cyclotron." in *Proc. Cyclotrons*. Vancouver, BC, Canada, 2013, p. 9.

[10] F. Haug *et al.*, "A small scale remote cooling system for a superconducting cyclotron magnet," in *Proc. IOP Conf. Series: Mater. Sci. Eng.*, Feb. 2017, vol. 171, Art. no. 012038.